

Figure 1. Structure of the TPHA zwitterion. **L** is the LC director and the rectangular, dashed frame represents the donor (-) and the acceptor (+) sites.

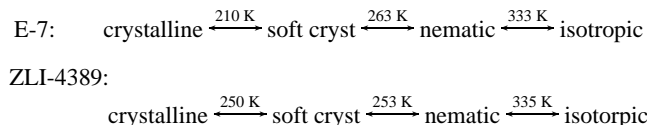
can be expanded over a wide temperature range (>120 °C), including ambient temperatures.¹ At such elevated temperatures the LC exhibits fluidlike properties, and the embedded chromophore's movements and orientations are restricted because of the LCs properties.^{16,17} Thus, when TPHA was dissolved in two different LCs and was photoexcited, TREPR was able to detect transient spectra which were typical of a radical pair (RP) state. Although photoinduced IET in zwitterionic systems has been previously examined by electronic spectroscopy,¹⁸ this is the first time the process has been monitored by TREPR.

In the present study, the chemical system and observations are unique with respect to a photochemical process, where the end product, a neutral RP, is formed by photoexcitation of the parent zwitterion, a charge separated ground state.

Experimental Section

The TPHA was synthesized as described elsewhere.¹⁵ The UV-vis spectrum was acquired with a HP 8452A diode array spectrophotometer with a 1 cm wide cell. The fluorescence measurements were measured at 90° geometry with a Spex Fluorolog spectrofluorometer with the appropriate correction file used for all emission spectra. All solvents used were distilled and solutions were freshly made for each emission measurement.

In the CW-TREPR experiments, toluene (Merck Ltd.) was dried over Na/K mirror overnight and was kept under vacuum throughout sample preparation. Two liquid crystals (LC) (Merck Ltd.) with different dielectric constants (E-7, $\epsilon = 19.0$; ZLI-4389, $\epsilon = 56$)¹⁹ were used and are characterized by the following phase transition temperatures:²⁰



Samples were first dissolved in toluene (~ 1 mM), which was then evaporated, and the LC was introduced into 4 mm OD pyrex tubes and degassed by several freeze-pump-thaw cycles on a vacuum line.

(16) Regev, A.; Levanon, H.; Murai, T.; Sessler, J. L. *J. Chem. Phys.* **1990**, *92*, 4718.

(17) Regev, A.; Galili, T.; Levanon, H. *J. Chem. Phys.* **1991**, *95*, 7907.

(18) Reichardt, C. In *Solvents and Solvent Effects in Organic Chemistry*, 2nd ed.; VCH: Weinheim, 1988; pp 285–291 and references therein.

(19) The chemical compositions are as follows: E-7 is an eutectic mixture of $R_1-C_6H_5-C_6H_5-CN$ where $R_1 = C_5H_{11}$ (51%), $R_2 = C_7H_{15}$ (25%), $R_3 = C_8H_{17}$ (16%), and $R_4 = C_5H_{11}C_6H_5$ (8%); the composition of ZLI-4389 is not available.

(20) The soft crystalline phase is an intermediate phase found in the vicinity of the melting point. It is characterized by some molecular motion of both the solvent and the solute. The transition temperatures of this phase may be estimated from the appearance of TREPR spectra that are the result of solvent-controlled electron transfer.

CW-TREPR measurements were carried out on a Varian E-12 spectrometer (X-band) in direct detection (DD) mode, interfaced to a pulsed dye-laser (Continuum TDL-60, 7 mJ/pulse, 560 nm wavelength at a repetition rate of 20 Hz) pumped by the second harmonic of a Nd:Yag laser (Continuum, 661-20). The response time of the EPR detection is ~ 200 ns. The temperature was controlled by a variable-temperature nitrogen-flow dewar inside the EPR resonator. Optical measurements were performed on a Hewlett-Packard UV-vis spectrophotometer in 2 mm wide quartz cells. Concentration of the samples was $\sim 10^{-4}$ M. The orientation of the LC director, **L**, with respect to the magnetic field, **B**, is determined by the sign of the diamagnetic susceptibility ($\chi_{||} - \chi_{\perp} = \Delta\chi$). In both LCs used here, $\Delta\chi$ is positive, and as a consequence, the default orientation is **L** || **B**. The EPR line shape analysis was carried out by using the density matrix formalism that has been described elsewhere.^{17,21} The uncertainty in the zero-field splitting parameters (ZFS) extracted from the line shape analysis and the relaxation times and electron-transfer rates from the kinetic analysis is $\pm 10\%$ and $\pm 15\%$, respectively.

The time profile of the magnetization, $M_y(t)$, was obtained by following the signal generated by the laser pulse at a specific magnetic field, under constant microwave irradiation. It should be noted that the observed EPR signals were completely reversible and did not show any saturation effect, thus by using high microwave power (100 mW) a substantial improvement of the signal-to-noise ratio was achieved. A detailed description of light excitation, signal detection, and data acquisition is given elsewhere.^{22–24} The EPR signal decay rates were extracted by analysis of the magnetization time profile, $M_y(t)$, using a previously derived biexponential expression:^{25–28}

$$M_y(t) = P_0\omega_1 \frac{[e^{-c_+t} - e^{-c_-t}]}{c_- - c_+} + \frac{P_{eq}}{T_1} \int_0^t \omega_1 \frac{e^{-c_+t'} - e^{-c_-t'}}{c_- - c_+} dt' \quad (3)$$

While the triplet kinetics are governed only by spin relaxation and microwave power, the RP kinetics also depend on the ET rate k_{ET} . Therefore, for best fit of triplet kinetics we have:

$$c_{\pm}^T = \frac{T_{2T}^{-1} + T_{1T}^{-1}}{2} \mp \left[\frac{(T_{2T}^{-1} - T_{1T}^{-1})^2}{4} - \omega_1^2 \right]^{1/2}$$

and for RP kinetics: c_{\pm}^{RP} :²⁷

$$c_{\pm}^{RP} = \frac{k'_{ET} + T_{1RP}^{-1}}{2} \mp \left[\frac{(k'_{ET} - T_{1RP}^{-1})^2}{4} - \omega_1^2 \right]^{1/2}$$

where $k'_{ET} = k_{ET} + 1/T_{2RP}$; T_{1T} , T_{1RP} , and T_{2T} , T_{2RP} are the respective spin-lattice and spin-spin relaxation times of triplet and radical pair, respectively; ω_1 is the microwave field; and P_0 and P_{eq} are the initial and equilibrium triplet state populations, respectively. The inhomogeneous broadening of the spectra is in the order of 10^6 s⁻¹, common to the triplet and RP dynamics. We also consider the contribution of T_{2RP} to the magnetization $M_y(t)$ of the RP by assuming comparable values for T_{2RP} and the rise time of the RP. Thus, the calculated value of k'_{ET} provides an upper limit for k_{ET} .

Results and Discussion

Figure 2 shows the absorption spectrum of TPHA dissolved in toluene at room temperature. It exhibits seven distinctive

(21) Gonen, O.; Levanon, H. *J. Phys. Chem. A* **1985**, *89*, 1637.

(22) Gonen, O.; Levanon, H. *J. Chem. Phys.* **1986**, *84*, 4132.

(23) Regev, A.; Berman, A.; Levanon, H.; Murai, T.; Sessler, J. L. *Chem. Phys. Lett.* **1989**, *160*, 401.

(24) Berman, A.; Levanon, H.; Vogel, E.; Jux, N. *Chem. Phys. Lett.* **1993**, *211*, 549.

(25) Hore, P. J.; McLauchlan, K. A. *J. Magn. Reson.* **1979**, *36*, 129.

(26) Hore, P. J. In *Advanced EPR Applications in Biology and Biochemistry*; Hoff, A. J., Ed.; Elsevier: Amsterdam, 1989; pp 405–440.

(27) Hasharoni, K.; Levanon, H.; von Gersdorff, J.; Kurreck, H.; Möbius, K. *J. Chem. Phys.* **1993**, *98*, 2916.

(28) It should be noted that eq 3 is valid if the formation of the paramagnetic species is faster and its decay is slower than the time dependence arising from spin relaxation and microwave excitation.

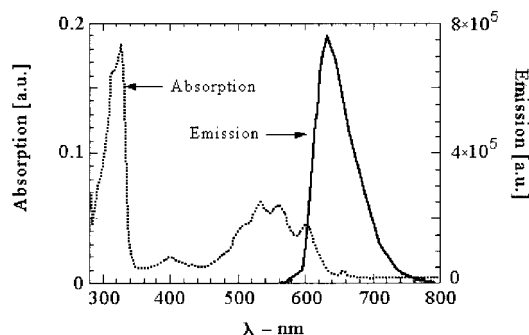


Figure 2. Absorption and emission spectra of TPHA in toluene at room temperature.

peaks ($\log \epsilon$): 314 (4.58), 328 (4.63), 400 (3.54), 510 (4.00), 533 (4.15), 560 (4.14), and 600 (3.99) nm. Laser excitation was carried out at 560 nm, which corresponds to one of the absorption maxima of TPHA. The emission spectrum of TPHA in toluene is also shown in Figure 2. The emission intensity was found to be sensitive to concentration quenching for concentrations $>10^{-5}$ M. Furthermore, the excitation profile varied with concentration and only emulated the UV-vis at concentrations $<10^{-5}$ M. We suspect these trends were due to aggregation of the TPHA in solution.²⁹ The emission wavelength (λ_{em}) was measured in toluene, ethyl ether, tetrahydrofuran, methylene chloride, ethanol, and acetonitrile. A blue shift in the emission wavelength was observed as the solvent's dielectric constant increased. The λ_{em} decreased from 633 nm in toluene ($\epsilon = 2.4$) to 618 nm in ethanol ($\epsilon = 25$) and acetonitrile ($\epsilon = 38$). The observed trend is the opposite that of anthracene and most fluorescent molecules, and suggests the ground state is more polar than the excited state.³⁰ The fluorescence results are in full agreement with eq 2, where the photoinduced biradical state (2) is expected to be less polar than TPHA in its ground state (1).

TREPR spectra at different temperatures (which correspond to different LC phases) of photoexcited TPHA oriented in ZLI-4389 are shown in Figure 3. The spectra were taken at the parallel, $L \parallel B$, and perpendicular, $L \perp B$, orientations, where L is the LC director and B is the external magnetic field. The time-resolved spectra are presented as a function of the time interval following the laser pulse. The spectra presented in this figure can be interpreted in terms of the molecular structure of TPHA (Figure 1) and the photochemical reaction scheme given in Figure 4.

The TREPR spectrum in Figure 3a (where $L \parallel B$) exhibits a relatively narrow line at $g \approx 2.009$ (peak-to-peak ~ 76 G) with an absorption/emission (a,e) phase pattern that does not change in time. This spectrum was simulated with the ZFS parameters, $|D| = 86$ G and $|E| = 0$. It should be noted that all magnetic and kinetic parameters of this signal are independent of the LC phase. The TREPR spectrum in the $L \perp B$ orientation is typified by two features: a broad polarized signal with a width of ~ 550 G (peak-to-peak), exhibiting an e,a phase pattern; and a narrow signal with a phase pattern a,e superimposed on the broad spectrum (Figure 3b). All magnetic parameters of the narrow and broad signals are the same as those observed in $L \parallel B$ orientation. The magnetization time profiles of the narrow and broad signals are shown in Figure 3, parts c and d, respectively. Despite the large difference in the dielectric constants and molecular structure of

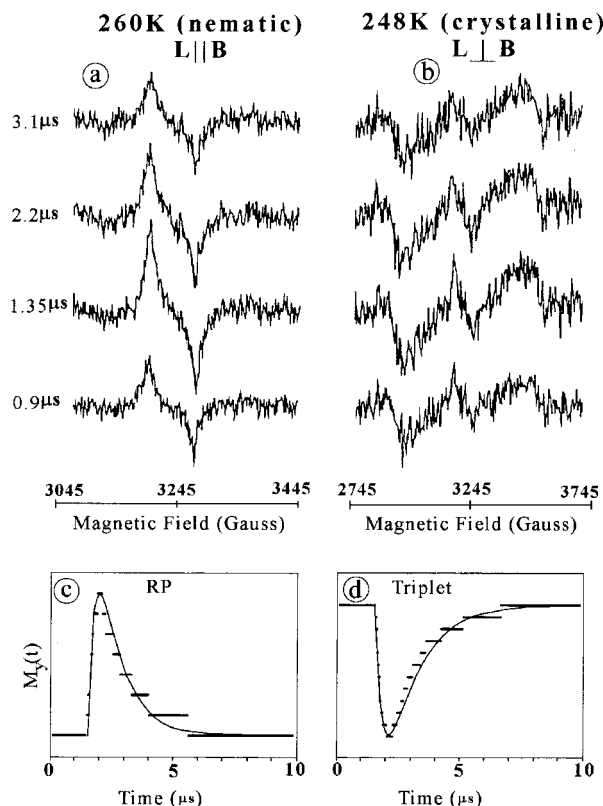


Figure 3. Top: TREPR spectra (direct detection) of TPHA in the different phases of LC (ZLI-4389), and different orientations of the sample with respect to the external magnetic field B . (a) $L \parallel B$; (b) $L \perp B$. The spectra at each temperature are presented as a function of the time interval following the laser pulse. Bottom: (c) Kinetic traces of the magnetization, $M_y(t)$, taken at the positive absorption of the RP. (d) Kinetic traces of the magnetization, $M_y(t)$, taken at the negative emission of the triplet spectrum. The dynamic parameters, $T_{1RP} = 0.79$ μ s, $T_{2RP} = 0.26$ μ s, $k'_{ET} = 7.3 \times 10^6$ s^{-1} (RP), $T_{1T} = 0.96$ μ s, and $T_{2T} = 0.36$ μ s (triplet), were extracted via the simulations by using eq 3.

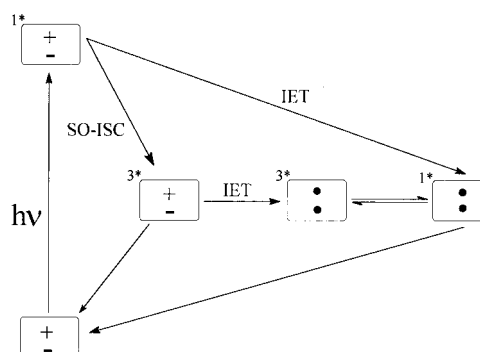


Figure 4. Scheme of the photochemical reactions in TPHA.

the two LCs employed, all magnetic and kinetic parameters extracted from the TREPR spectra were found to be practically identical and are temperature independent. On the other hand, the signal-to-noise ratio in the ZLI-4389 LC was found to be higher than that in the E-7 LC.

It is reasonable to attribute the broad spectrum in Figure 3b is that of a triplet state, $3^*[\pm]$, which is obtained via spin-orbit intersystem crossing (SO-ISC), as shown in Figure 4. These spectra can be simulated with the ZFS parameters, $|D| = 296$ G and $|E| = 94$ G. The e,a phase pattern can be accounted for in terms of spin-selective ISC to the $|x\rangle$, $|y\rangle$, and $|z\rangle$ zero-field spin levels with relative population rates: $A_x = 1.0$; $A_y = 0.8$; $A_z = 0.0$ (x and y axes lie in the molecular plane). In labeling

(29) Shoemaker, D. P.; Garland, C. W.; Nibler, J. W. *Experiments in Physical Chemistry*, 5th ed.; McGraw-Hill: New York, 1989.

(30) Guilbault, G. G. *Practical Fluorescence Theory, Methods and Techniques*; Marcel Dekker: New York, 1973.

the EPR transitions it has been assumed that $D > 0$, as is normally the case for π^* triplets, and that the relative order of triplet spin levels is $|x\rangle > |y\rangle > |z\rangle$.²² The simulations of the triplet EPR spectra also provide the fluctuation angle between the LC director and the in-plane molecular axis, with a peak probability at some angle ϕ_0 (Figure 1). Attempts to observe changes in the line shape by changing the direction of light polarization via a magnetophotoselection experiment^{31,32} resulted in the same triplet EPR spectra for both directions of light polarization. Such a result should provide valuable information on the direction of the optical transition moment and the absolute sign of the ZFS parameter, D .³³ Unfortunately, the poor signal-to-noise ratio of the triplet spectra does not allow an unambiguous conclusion concerning this point.

Previously reported calculations¹⁵ on TPHA have predicted the triplet structure **2** to consist of two delocalized spins approximately 7 Å apart. Such a short distance gives a strong exchange interaction, J , resulting in separation between the singlet and triplet manifolds, which reduces the amount of S–T mixing. Therefore, and similar to previous studies,^{5,27} the EPR signal is attributed to a triplet RP, $^3[{}^{\pm}]$. If indeed this is the case, the interrational distance (r) can be estimated by the point dipole approximation by using the ZFS parameters calculated by the line shape analysis of the triplet RP spectra in Figure 3. Thus, from the relation $D = 3/4[(g\beta)^2/r^3]$, where g is the g factor, β is the Bohr magneton, r is in Å, and D is in G, a value of $r = 6.8$ Å is obtained, which is in excellent agreement with the distance predicted by theory.

(31) Thurnauer, M. C.; Norris, J. R. *Biochem. Biophys. Res. Commun.* **1976**, *73*, 501.

(32) Regev, A.; Michaeli, S.; Levanon, H.; Cyr, M.; Sessler, J. L. *J. Phys. Chem. A* **1991**, *95*, 9121.

(33) Frank, H. A.; Bolt, J.; Friesner, R.; Sauer, K. *Biochim. Biophys. Acta* **1979**, *547*, 502.

The origin of the RP can either be the triplet, $^3[{}^{\pm}]$, or the singlet, $^1[{}^{\pm}]$, as seen in Figure 4. Comparison of the decay time of the triplet magnetization (ca. 1.3 μ s) and the rise time of the RP signal (ca. 0.3 μ s) leads us to conclude that the triplet state, $^3[{}^{\pm}]$, of TPHA is not the precursor of the RP (Figure 4). Thus, the triplet radical pair is formed by an IET from the singlet excited state, $^1[{}^{\pm}]$ (Figure 4). The relatively short distance between the donor and acceptor sites does not allow for a vanishing J value. Thus, it is reasonable to assume that $|S\rangle$ is located in the vicinity $|T_{-}\rangle$ which results in efficient S–T–mixing.²⁷ Therefore as expected, for a $D < 0$, such S–T–mixing will result in the selective populations of T_{\pm} which will be reflected by an a,e polarization pattern.²⁷

In conclusion, we are the first to report TREPR of an IET in a zwitterionic molecule, which demonstrates that photoexcitation of a charge separated ground state results in a neutral biradical via an excited singlet state. An integral part of these novel observations is the role of the LC, whose properties are critically essential that such experiments will be successfully accomplished.

Acknowledgment. This work was supported by the U.S.-Israel BSF, the Deutsche Forschungsgemeinschaft (Sfb 337), and a grant from the Ministry of Science in Israel and Forschungszentrum Juelich GmbH (KFA) in Germany. The Farkas Center is supported by the Bundesministerium für die Forschung und technologie and the Minerva Gesellschaft für Forschung GmbH, Germany. We thank the National Science Foundation for support through the MRSEC and grant DMR-9500888 as well as the Air Force Office for Scientific Research through a grant. K.A.H. thanks the DOD for a National Defense Science and Engineering Graduate Fellowship and Chris Brown.

JA974018U